



## Comparative toxicity evaluation of flowershaped and spherical gold nanoparticles on human endothelial cells

Sadequa Sultana, Nadia Djaker, Sanda Boca-Farcau, Milena Salerno, Nathalie Charnaux, Simion Astilean, Hanna Hlawaty, Marc Lamy de La Chapelle

### ► To cite this version:

Sadequa Sultana, Nadia Djaker, Sanda Boca-Farcau, Milena Salerno, Nathalie Charnaux, et al.. Comparative toxicity evaluation of flowershaped and spherical gold nanoparticles on human endothelial cells. Journées RITS 2015, Mar 2015, Dourdan, France. Actes des Journées RITS 2015, p22-24 Section nanomédecine. <inserm-01145552>

**HAL Id: inserm-01145552**

**<http://www.hal.inserm.fr/inserm-01145552>**

Submitted on 24 Apr 2015

**HAL** is a multi-disciplinary open access archive for the deposit and dissemination of scientific research documents, whether they are published or not. The documents may come from teaching and research institutions in France or abroad, or from public or private research centers.

L'archive ouverte pluridisciplinaire **HAL**, est destinée au dépôt et à la diffusion de documents scientifiques de niveau recherche, publiés ou non, émanant des établissements d'enseignement et de recherche français ou étrangers, des laboratoires publics ou privés.



Distributed under a Creative Commons Attribution 4.0 International License

## Comparative toxicity evaluation of flowershaped and spherical gold nanoparticles on human endothelial cells

Sadequa Sultana<sup>1</sup>, Nadia Djaker<sup>1\*</sup>, Sanda Boca-Farcau<sup>2</sup>, Milena Salerno<sup>1</sup>,  
Nathalie Charnaux<sup>3</sup>, Simion Astilean<sup>2</sup>, Hanna Hlawaty<sup>3</sup> and  
Marc Lamy de la Chapelle<sup>1</sup>

<sup>1</sup>Université Paris 13, Sorbonne Paris Cité, UFR SMBH, Laboratoire CSPBAT, CNRS (UMR 7244), 74 rue Marcel Cachin, F-93017 Bobigny, France.

<sup>2</sup>Babes-Bolyai University, Institute for Interdisciplinary Research in Bio-Nanoscience and Faculty of Physics, Nanobiophotonics and Laser Microspectroscopy Center, 1 Str. M Kogalniceanu, RO-400084 Cluj- Napoca, Romania.

<sup>3</sup>Université Paris 13, Sorbonne Paris Cité, UFR SMBH, INSERM U1148, Laboratory for Vascular Translational Science, Bio-ingénierie cardio-vasculaire, 74 rue Marcel Cachin, F-93017 Bobigny, France.

\*nadia.djaker@univ-paris13.fr

**Abstract** – *In this work, we propose a multi-parametric in vitro study of the cytotoxicity of gold nanoparticles (GNPs) on human endothelial cell (HUVEC). The cytotoxicity is evaluated by incubating cells with six different GNP types which have two different morphologies: spherical and flower-shaped, two sizes (~15 and ~50 nm diameter) and two surface chemistries (as prepared form and PEGylated form). Our results showed that by increasing the concentration of GNPs the cell viability decreases with a toxic concentration threshold of 10 pM for spherical GNPs and of 1 pM for flower-shaped GNPs. Dark field images, flow cytometry and spreading test revealed that flower-shaped GNPs have more deleterious effects on the cell mechanisms than spherical GNPs. We demonstrated that the main parameter in the evaluation of the GNPs toxicity is the GNPs roughness and that this effect is independent on the surface chemistry. We assume that this behavior is highly related to the efficiency of the GNPs internalization within the cells and that this effect is enhanced due to the specific geometry of the flower-shaped GNPs.*

**Index terms** - *Microscopy, Nano medicine, Optical Imaging.*

### I. INTRODUCTION

Gold nanoparticles (GNPs) are of great interest for several applications in nanomedicine, especially in imaging and sensing [1], drug delivery [2, 3] and photothermal therapy [4, 5] because of their unique physical and chemical properties, and high biocompatibility.

Among different morphologies of GNPs, gold nanospheres (GNSs) are widely used for biomedical applications [6, 7]. In recent years, gold nano flowers (GNFs) (also termed as urchin like, branched particles or stars) have been proposed to improve the light-matter interaction and thus the optical properties of such nanostructures which is essential for photothermal

therapeutics [8, 9] or optical cellular imaging [10–12]; thanks to their tips which are responsible to a higher local electromagnetic field enhancement [13].

For all these applications, a better understanding of the interaction and uptake of GNPs into cells is of great importance and currently under intense investigation [14–17], especially for GNFs who exhibit improved optical properties. In this latter case, it is then of first importance to determine if this higher efficiency is suitable with an acceptable biocompatibility. variable in their interaction with cells [18–20]. Chithrani et al reported the effect of GNP size on the cellular uptake with sizes varying between 14 and 100 nm [21]. GNPs larger than 10 nm in diameter internalized inside cells were trapped in vesicles in the cytoplasm and did not enter in the nucleus [18, 21]. Pan et al suggested that the uptake of GNPs is mediated by non-specific adsorption of proteins onto the gold surface, which induces internalization into cells via the endocytosis mechanism [19, 20].

Many reported works showed that GNPs size and aggregation can affect cell adhesion and proliferation: Cui et al showed that small GNSs (2 nm), which are more stable against aggregation, caused less HeLa cytotoxicity than larger GNSs (25 nm) which are liable to form aggregates [22]. Arvizo et al studied the effect of GNP size on inhibition of endothelial and fibroblast cell proliferation. It was demonstrated that 20 nm GNSs showed a maximal inhibition of cell proliferation up to 100% whereas 10 nm showed up to 60% and 5 nm up to 25% of inhibition [23]. In the same way, Pernodet et al reported that 14 nm GNSs had a significant uptake into dermal fibroblasts [24]. It was suggested that the presence of GNPs is responsible for abnormal actin filaments and extracellular matrix constructs in dermal fibroblasts; which decrease cell proliferation, adhesion, and motility. Jiang et al proposed that GNPs can not only passively interact with cells, but also at a specific size actively alter the molecular processes that are essential for regulating the cell functions [25]. GNPs of 40–50 nm are found to be the optimal sizes for receptor-mediated endocytosis. This

higher particle uptake is probably due to the direct balance between multivalent cross linking of membrane receptors and the process of membrane wrapping involved in receptor-mediated endocytosis.

Nanoparticle size is not the only relevant parameter in the GNPs–cell interaction. The cell membrane seems to be also very sensitive to the GNP's surface chemistry. By considering only the surface chemistry, Goodman et al found that cationic particles are moderately toxic, whereas anionic particles are rather less toxic [18, 26]. Freese et al have discussed different polymer coatings and concluded that the positive-charge coated GNPs were internalized to a greater extent than the negative- or neutral-charged GNPs, as would be expected due to interactions with the anionic cell membrane [27]. Arnida et al showed that GNPs appeared to be taken up by nonspecific adsorptive endocytosis [28]. PEGylation (PEG=poly ethylene glycol) on the surface of GNPs drastically reduced this uptake.

In this study, we have employed such approach to evaluate the cellular uptake and cytotoxicity of GNPs in adherent human endothelial cells (HUVEC). Our study includes in total six different types of GNPs which have two morphologies: spherical (~15 and ~50 nm diameter termed as: 15-a-GNS and 50-a-GNS) and flower-shaped (only ~50 nm diameter termed as: a-GNF); and two surface chemistries- as prepared form and after polymer stabilization by polyethylene glycol which were termed as: 15-PEG-GNP, 50- PEG-GNP, PEG-GNF.

## II. MATERIALS AND METHODS

### II.1. Synthesis and surface modification of GNPs

GNFs were prepared by the rapid mixture of 20 mL solution of  $19.8 \times 10^{-3} \text{M}$  of ascorbic acid with 200  $\mu\text{l}$  of  $10^{-2} \text{M}$  of  $\text{HAuCl}_4$  at ice temperature [12]. Colloidal GNSs of 15 nm were synthesized by the aqueous reduction of  $\text{HAuCl}_4$  with trisodium citrate according to the Turkevich–Frens method.

One batch of each type of GNPs was modified using mPEG-SH polymer of 5 kDa molecular weight, that provided more stability to the particles. Depending on the nanoparticle type and hence on its surface area, various amounts of  $10^{-3} \text{M}$  polymeric solution were added to the colloidal solution by dripping. The polymer-nanoparticle mixtures were subjected to vigorous stirring after which let to sit for 24 h at 4 °C to afford a complete binding of the polymer. Both as-prepared and polymer stabilized GNPs (a-GNPs and PEG-GNPs, respectively) were purified by centrifugation at high speed and resuspended in ultrapure water until the incubation with cells.

### II.2. Cell culture

Human vascular endothelial cells (HUVEC, N CRL-1730, ATCC, LGC Molsheim, France) were cultured in endothelial cell basal media 2 (ECBM2, PromoCell, Germany) supplemented with 10% fetal bovine serum, epidermal growth factor (EGF, 5.0 ng mL<sup>-1</sup>),

hydrocortisone (0.2  $\mu\text{g mL}^{-1}$ ), VEGF (0.5 ng mL<sup>-1</sup>), basic fibroblast factor (bFF, 10 ng mL<sup>-1</sup>), insulin like growth factor (R3IGF-1, 20 ng mL<sup>-1</sup>), ascorbic acid (1  $\mu\text{g mL}^{-1}$ ), heparin (22.5  $\mu\text{g mL}^{-1}$ ), antibiotics (penicillin-streptomycin, 1, Invitrogen, France) and L-glutamine (1, Invitrogen, France) at 37 °C. in 5% CO<sub>2</sub>.

## III. RESULTS & DISCUSSION

Figure 1 illustrates the results of cell morphology, actin cytoskeleton structure and histograms of measured cell surface area of blank and treated cells with GNPs. In control condition (figure 1(A)) of non-treated HUVEC, fluorescence microscopy images showed F-actin fibers (with rhodamine-labeled phalloidin) in whole cell body and in adhesion focal contacts. The cells had well spread form showing cell-to-cell or cell-to-extracellular matrix focal adhesion complex (FAC). F-actin fibers had continuous thread-like structure which seemed nicely distributed along the cell body giving to the endothelial cell an appropriate regular morphology (not deform, not compact cell shape, well spread shape).

In the case of treated cells with GNSs, coexistence of both deformed and few spread cells with healthy structure are observed (figures 1(B1) and (C1)); whereas, treated cells with GNFs showed more deformed and compact cells with a highly concentrated actin fibers in cell peripheries (figure 1(D1)). In general, we observe that F-actin cytoskeleton of all GNPs treated cells has been alternated compared to blank, well spread cells showing the stress fibers formation.

After 3 h incubation with GNPs, the cell surface areas were measured for 100 cells from both GNPs treated and nontreated (blank) cells and represented as histograms to elaborate quantitatively the extent of changes in cell morphology. Thus it fully represents the stress caused by the presence of GNPs. The mean cell surface area of 50-PEG-GNSs treated cells is around 540  $\mu\text{m}^2$  whereas for 50-a-GNSs, the cell surface area is about 420  $\mu\text{m}^2$  (figure 1(B2)). In the case of 15-PEGGNSs, the mean surface area of treated cells was around 440  $\mu\text{m}^2$ , while for 15-a-GNSs it was close to 340  $\mu\text{m}^2$  (figure 1(C2)). GNFs exhibited a prominent shape effect on the cell surface area (figure 1(D2)). For both surface chemistries the surface area was reduced to 350  $\mu\text{m}^2$  for PEGGNFs and to 260  $\mu\text{m}^2$  for a-GNFs. Therefore, comparing to control (650  $\mu\text{m}^2$ ), the loss in cell surface area was in order of a-GNFs (60%) > 15-a-GNSs (48%) > 50-a-GNSs (35%).

This observation can also be done for all PEG-GNPs such as the loss in cell surface is estimated to be PEG-GNFs (46%) > 15- PEG-GNSs (32%) > 50-PEG-GNSs (17%). Thus, a decrease of the surface area of the cells is observed for all the GNPs and all surface chemistry. This indicate that whatever the GNPs used, the cells are stressed even if this effect is reduced by the used of PEGylated surface chemistry and by the use of 50-GNS.

Furthermore, we observe the same hierarchical organization of the effects as for previous experiments (cell viability) meaning the highest effect for the a-GNF and the lowest one for the 50-PEG-GNS.

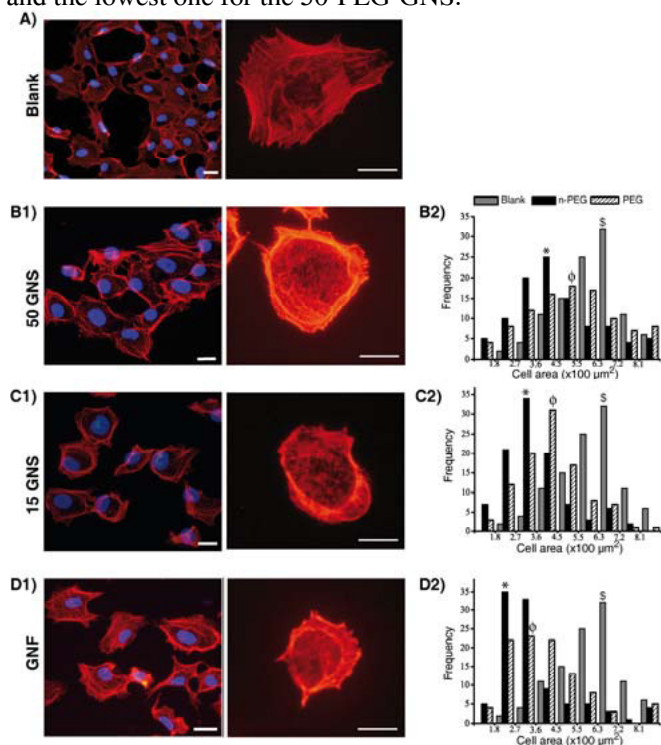


Figure 1: Fluorescence images of HUVEC incubated with 0.5 pM of GNPs for 3 h (A: blank, B1: 50-a-GNS, C1: 15-a-GNS and D1: GNF) (scale bar: 7  $\mu$ m). Nuclei are labeled with DAPI (blue) and actin cytoskeleton with Alexa Fluor 546-phalloidin (orange-red). Histograms represent the cell surface areas of control cells (gray) and cells incubated with (B2) 50-GNS, (C2) 15-GNS and (D2) GNF. In histograms, black and striped bars demonstrate consecutively as prepared and PEG surface chemistries of the GNPs. Moreover, \$ denotes average cell area of cells in blank, \* and  $\phi$  denote the average surface area of as prepared and PEG-GNPs treated cells respectively.

#### IV. CONCLUSION

In this work, we demonstrate that the cytotoxicity of the GNPs depends on the size and the shape of the GNPs as well as on the surface chemistry. Increasing concentration of nanoparticles decreased cell viability; and thus we determined the threshold toxic concentration of around 100 pM, 10 pM and 0.5 pM consecutively for 50-a-GNSs, 15-a-GNSs and a-GNFs. Flow cytometry analysis demonstrated the more deleterious effect of GNFs over GNSs. We noticed more affinity of GNFs on HUVEC than 15-GNSs, where 50-GNSs had the least affinity. We were able to compare the degree of cytotoxic effect and demonstrated that it is largely higher for GNFs than for GNSs. Even if we showed an enhanced biocompatibility of the GNSs due to the PEG coating, we demonstrated that the surface chemistry has no effect for the GNFs. This latter point indicates that the main parameter in the

evaluation of the GNPs toxicity is the GNPs roughness. Thus, even if the GNFs have optical properties that imply a better efficiency in application as photothermal therapy, they could have more deleterious effects on the biological media.

#### ACKNOWLEDGMENTS

This work has been supported by the Region Ile-de-France in the framework of DIM C'Nano IdF and 'Nanosciences in Ilede-France'.

#### REFERENCES

- [1] Ricketts K, Castoldi A, Guazzoni C, Ozkan C, Christodoulou C, Gibson A P and Royle G J 2012 Phys. Med. Biol. 57 5543
- [2] Paciotti G F, Myer L, Weinreich D, Goia D, Pavel N, McLaughlin R E and Tamarkin L 2004 Drug Deliv. 11 169–83
- [3] Amitava D, Priyabrata M, Sumit K S, Praveen G, Megan C F, Debabrata M, Vijay H S and Chitta Ranjan P 2010 Nanotechnology 21 305102
- [4] De Freitas L F et al 2013 Laser Phys. 23 066003
- [5] Boris K, Vladimir Z, Andrei M, Valery T and Nikolai K 2006 Nanotechnology 17 5167
- [6] Huang X, Jain P K, El-Sayed I H and El-Sayed M A 2007 Nanomedicine 2 681–93
- [7] Jain P K, Lee K S, El-Sayed I H and El-Sayed M A 2006 J. Phys. Chem. B 110 7238–48
- [8] Yuan H, Khoury C G, Wilson C M, Grant G A, Bennett A J and Vo-Dinh T 2012 Nanomedicine: NBM 8 1355–63
- [9] De Broek B V, Frederix F, Bonroy K, Jans H, Jans K, Borghs G and Maes G 2011 Nanotechnology 22 015601
- [10] Rodríguez-Lorenzo L, Krpetic Z, Barbosa S, Alvarez-Puebla R A, Liz-Marzán L M, Priore I A and Brust M 2011 Integr. Biol. 3 922–6
- [11] Yuan H, Fales A M, Khoury C G, Liu J and Vo-Dinh T 2013 J. Raman Spectrosc. 44 234–9
- [12] Boca S, Rugina D, Pinteá A, Barbu-Tudoran L and Astilean S 2011 Nanotechnology 22 1–7
- [13] Sau T K, Rogach A L, Jäckel F, Klar T A and Feldmann J 2010 Adv. Mater. 22 1805–25
- [14] Alkilany A M, Nagaria P K, Hexel C R, Shaw T J, Murphy C J and Wyatt M D 2009 Small 5 701–8
- [15] Bartczak D, Muskens O L, Nitti S, Sanchez-Elsner T, Millar T M and Kanaras A G 2012 Small 8 122–30
- [16] Soenen S J, Rivera-Gil P, Montenegro J-M, Parak W J, De Smedt S C and Braeckmans K 2011 Nano Today 6 446–65
- [17] Raja G R, Wilma P, Liesbeth H, Patrick C, Hans J, Fijs W B V L, Cees O, Srirang M and Ton G V L 2010 Nanotechnology 21 145101
- [18] Connor E E, Mwamuka J, Gole A, Murphy C J and Wyatt M D 2005 Small 1 325–7
- [19] Díaz B et al 2008 Small 4 2025–34
- [20] Pan Y, Neuss S, Leifert A, Fischler M, Wen F, Simon U, Schmid G, Brandau W and Jahnen-Dechent W 2007 Small 3 1941–9
- [21] Chithrani B D, Ghazani A A and Chan W C W 2006 Nano Lett. 6 662–8
- [22] Cui W, Li J, Zhang Y, Rong H, Lu W and Jiang L 2012 Nanomedicine: NBM 8 46–53
- [23] Arvizo R R, Rana S, Miranda O R, Bhattacharya R, Rotello V M and Mukherjee P 2011 Nanomedicine: NBM 7 580–7
- [24] Pemodet N A F, X H, Sun Y, Bakhtina A, Ramakrishnan A, Sokolov J, Ulman A and Rafailovich M 2006 Small 2 Q3 766–73
- [25] Jiang W, Kim B Y S, Rutka J T and Chan W C W 2008 Nat. Nanotechnology 3 145–50
- [26] Shukla R, Bansal V, Chaudhary M, Basu A, Bhonde R R and Sastry M 2005 Langmuir 21 10644–54
- [27] Freese C, Gibson M I, Klok H-A, Unger R E and Kirkpatrick C J 2012 Biomacromolecules 13 1533–43
- [28] Arnida M A and Ghandehari H 2009 J. Appl. Toxicol. 30 212–7